

Orientation dependent handedness and chiral design

Efi Efrati* and William T. M. Irvine

*James Franck Institute,
The university of Chicago. 929 E. 57 st,
Chicago, IL 60637,
USA*

Chirality occupies a central role in physical and material science: from colloidal and biological self assembly to the design of optical meta-materials. The definition of chirality, as given by lord Kelvin, associates handedness with the lack of mirror symmetry: the inability to superpose an object on its mirror image. While this definition has guided the classification of chiral objects for over a century, the quantification of chiral *phenomena* based on this definition has proven elusive, if not impossible as manifest in the paradox of chiral connectedness. In this work we put forward a quantification scheme in which the chirality of an object depends on the direction in which it is viewed. While consistent with familiar chiral notions, such as the right hand rule, this framework allows objects to be simultaneously right and left handed. We demonstrate this orientation dependence in three different systems: a biomimetic elastic bilayer, a chiral propeller and a chiral optical meta-material and find quantitative agreement with chirality pseudo-tensors whose form we explicitly compute. The use of this approach resolves the existing paradoxes and naturally enables the design of chiral meta materials from symmetry principles.

Chiral phenomena often span many length scales. The distinct handedness displayed by the proteinogenic amino acids persists over nine orders of magnitude and manifests in the full organism scale (4), for example by positioning our hearts on the left. As the forces holding the building blocks of our body together are symmetric under reflection, had the amino acids opposite handedness so would have the positioning of the our visceral organs (5). This suggests a connection between the chirality of a body and that of its constituents. Quantifying this connection, however, has proven to be highly non-trivial even when considering relatively simple systems.¹

Associating a number with the chirality of an object such that it is consistent with lord Kelvin's definition - *i.e.* that it change sign under reflections (transform as a pseudo-scalar) and vanish only for bodies which are mirror symmetric (superposable on their own mirror image)² - has proven to be an impossible task (3; 7). This is because it is always possible to continuously deform a body into its mirror image without passing through a configuration which is mirror symmetric³. It follows that all scalar chiral measures either possess false zeros (assign a

vanishing chirality to objects which are not mirror symmetric) or are not pseudo-scalar. Many operational measures, such as the optical activity of an isotropic body, are naturally pseudo-scalar and therefore must possess false zeros; for this reason they have been argued to be inadequate (8). In order to avoid false zeros chirality "degree" measures, which do not change sign under reflections, have been defined (3). Examples include measuring the distance (with respect to a configurational metric) of an object from its mirror image (9) or from the closest mirror symmetric body (10). It is however unclear how these chirality degree measures relate to physically measurable chiral quantities.

In Lord Kelvin's definition of chirality the lack of mirror symmetry (which is synonymous with broken parity symmetry), is taken to be the essential ingredient. The ability to assign either a left or right handedness to an object is, however, not captured by this definition of chirality. In this letter we show that adopting the physicists notion of handedness as a relation between directions and rotation leads to naturally tensorial and thus orientation dependent measures of chirality. While isotropic averages of these measures recover Kelvin's definition, the full measures predict orientation-dependent chiral behavior even for objects that are mirror symmetric. This orientation dependent approach is made quantitative, applied to experiments and shown to provide a natural tool for the design of chiral meta-materials.

Figure 1 shows a thin elastic bi-layer whose internal structure is homogeneous in the plane and symmetric under reflections. When long and narrow strips are cut from the bilayer they curve to form helicoidal strips of both right and left handedness depending on the relative orientation of the strips and the directions in which the layers were stretched. The handedness of each of the

* efrati@uchicago.edu

¹ For example, Straley (6) showed that simple steric interactions can drive right handed "screw like" molecules to stack in both right handed and left handed fashions depending on the relative values of the microscopic pitch and the molecular diameter.

² Such bodies are sometimes called achiral or amphichiral. The group of mirror symmetric object contains the subset of objects that possess symmetry under reflections, and the subset of objects which possess symmetry under inversions.

³ This property, known as chiral connectedness holds for all three dimensional bodies possessing five or more degrees of freedom, in particular all continuous bodies.

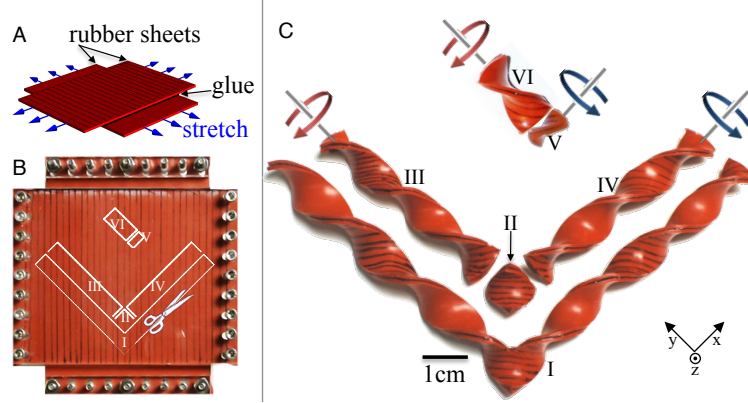


FIG. 1 *Orientation dependent manifestation of chirality in a reflection symmetric continua.* Two identical rubber sheets are uniaxially stretched and glued together to form a rubber bilayer as done in (11). Narrow strips cut from the bilayer curve out of plane to accommodate the difference in rest length between the layers and form helical structures. The square boundaries in b.II give rise to a cutout c.II which is symmetric under reflections. This is a manifestation of the symmetry of the bilayer's intrinsic structure. If, however, the cutout boundaries do not respect the bi-layer's symmetry, e.g. b.III and b.IV, strips with a well defined handedness result, as seen in c.III, and c.IV. The handedness observed depends solely on the orientation of the strip's long axis; strips aligned with one diagonal generate right handed helicoids, whereas strips oriented in the perpendicular direction generate left handed helicoids. Slicing a narrow piece from a left handed strip such that its aspect ratio is inverted yields a narrower strip of opposite handedness as seen in c.V which was cut from c.VI.

The square cutout c.II holds the capacity to generate both right and left handed strips. We thus consider it as possessing both right and left handedness in equal amounts rather than being achiral. It is right handed along the x direction, and left handed along the y direction. This directional dependence of the chirality is also observed in the relative positioning of cut-outs c.II, c.III and c.IV where the symmetric cutout c.II can be seamlessly continued in to manifestly Right or Left handed helical structures. Such an oriented dependant chirality cannot be captured by any pseudo-scalar measure and calls for quantification by a pseudo-tensor.

helicoidal strips is easily determined by following the surface's face with the right hand. If advancing along the helicoid's length requires the hand to roll outward, the helicoid is said to be right-handed (see for example the helicoidal strip in Figure 1 C.IV).

As the orientation of the boundary of a given cutout together with the intrinsic structure of the bi-layer break the bi-layer's mirror symmetry, one may argue that the appearance of handedness is to be expected. However, further examination reveals that even the cutouts that possess mirror symmetry (such as the cutout c.II) display one handedness in the $\pm x$ directions and the opposite handedness in the $\pm y$ directions.

Neither (pseudo-)scalars nor (pseudo-)vectors are capable of capturing this behaviour. The simplest object that captures such an orientational variation is a (rank 2) pseudo-tensor such as the one shown in Eq. 1:

$$\mathcal{X} = c \begin{pmatrix} 1 & 0 & 0 \\ 0 & -1 & 0 \\ 0 & 0 & 0 \end{pmatrix}. \quad (1)$$

This pseudotensor is symmetric under reflection, associates the x direction with a right (+) handed rotation about the x axis, and associates the y direction with a left handed rotation (-) about the y axis.

The notion of handedness employed above can be captured by an orientation dependent chirality pseudo-tensor density, χ^e . For every two unit vectors $\hat{\mathbf{n}}$ and $\hat{\mathbf{m}}$ we take the contraction $\hat{\mathbf{m}}\chi^e\hat{\mathbf{n}}$ to quantify the rotation of the surface's normal about the vector $\hat{\mathbf{m}}$ when it is displaced along the surface in the direction projected from $\hat{\mathbf{n}}$. It will be positive if the rotation about $\hat{\mathbf{m}}$ is right handed and negative when the associated rotation is left handed. This chirality density, similar in spirit to the tensorial measure proposed in (12), can be given explicitly in terms of the surface's fundamental forms (see appendix) and may be integrated to give a tensorial chiral measure of the surface as a whole: $\mathcal{X}_{ij}^e = \iint \chi_{ij}^e dA$. For example, calculating \mathcal{X}^e for the symmetric cutout in figure 1 c.II yields a chirality tensor of the form given in Eq. (1), as expected from its symmetry, with $c = 14 \text{ mm}^{-1}$.

When the same measure applied above to a mirror symmetric object is applied to the elongated helicoidal strips, IV and III, it gives rise to diagonal chirality tensors with the diagonal components $(88, -44, -44) \text{ mm}^{-1}$ and $(44, -88, 44) \text{ mm}^{-1}$ respectively. These tensors are no longer mirror symmetric, but are mirror images of each other and traceless. The latter is because every local measure of handedness on strictly 2D surfaces (containing no additional structure) gives rise to a symmetric and traceless rank two pseudo-tensor (see SM7 for proof).

Tensorial measures need not in general be the result

linear summation from a local density, and may not be available in explicit form. Nonetheless, the different tensor components may be probed operationally. An example of this, is provided by the experiment reported in Figure 2, which shows a section of a right handed helicoid that was constrained to rotate about each of two perpendicular axes and subjected to an airflow along the constraint axis. When constrained along its longest direction, the flow induced a left handed rotation, as expected. When constrained to rotate about the perpendicular direction, the same flow induced a (faster) *right*-handed rotation.

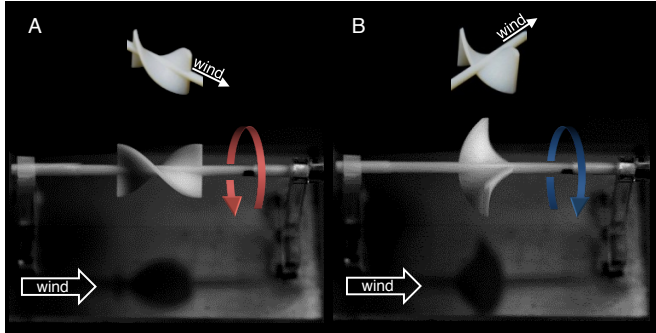


FIG. 2 *Probing the different components of chirality: Air flow past a helicoid.* Two identical right handed helicoidal surfaces, supported by thin cylindrical rods oriented along perpendicular directions display opposite response to airflow. The helicoids were printed using a three-dimensional printer (Objet Connex350TM) and measure 2cm wide and π cm long. The axis of the first helicoid is oriented along its length (**a**), whereas the axis of the second helicoid is oriented along the traverse direction (**b**). The structures were placed in an airflow and their axes hinged to allow free rotation about the direction of flow. (**a**) As air flows past the longitudinal axis of the helicoid, the latter rotates in a left handed fashion. (**b**) The same helicoid rotates in right-handed fashion when hinged along the perpendicular direction. Surprisingly, the helicoid hinged along the traverse direction rotates faster than the one hinged along its long axis.

As a third and final example of the application of tensorial measures in capturing chiral behavior we now consider optical scattering. Traditionally, optical scattering has been used as a probe for the chiral shape of invisible molecules, the implicit assumption being the existence of a direct connection between a ‘chiral’ electronic shape of each molecule, randomly oriented in solution, and the rotation of the polarization of light traveling through the solution. The manifestation of any handed phenomena in such isotropic collections of molecules necessitates the absence of mirror symmetry. For non-isotropic structures, however, this is not the case as observed by the optical activity of the mirror symmetric crystal of Silver Gallium Sulphide (14). Recently, in designing optical meta-materials it has become possible to consider scatterers, including mirror symmetric ones, at fixed ori-

entations. One of the key questions is to understand the relation between the shape of these scatterers and functional optical response. In attempts to design tunable optically active meta-materials, recent experiments have measured the orientationally varying optical activity when microwave radiation was scattered off planar arrays of planar structures (15). The planar structure, which is constructionally favorable, automatically renders the scatterers mirror symmetric. We point out here that the full orientation-dependent response of such reflection symmetric structures can be deduced from the measurement of the response at a single orientation by encoding the symmetry of the scatterers in a chirality tensor. As in the case of mirror symmetric objects considered above the symmetry of planar scatterers in fact implies a rank 2 chirality response tensor of the form appearing in Eq.1.

To further study the applicability of this approach, we carry out numerical calculations of scattering of microwave radiation from thin conducting semi-circular wires. The scatterer considered in Figure 3(a) is symmetric under reflection (about two perpendicular planes) and planar, rendering it similar to bent core molecules which form polar nematic phases, and were recently shown to exhibit an isotropic chiral liquid crystal phase (16). Figure 3 shows the optical activity of the scatterer computed numerically (see SM3 for details). As observed in the experiments of (15), the scatterer displays both right and left handed optical activity depending on its orientation relative to the exciting k vector. To within small contributions of higher order tensors (whose orientational variation is calculated explicitly in SM10), the optical activity obeys the form of Equation (1). It is therefore completely determined by a single response curve, and displays an angular dependance which scales with $\sin(2\alpha)$ where α is the angle between the normal to the scatterer plane and the k vector. Rescaling by this factor yields the collapse observed in Figure 3(a).

This approach has immediate applications in meta-material design, for example in the design of a purely optically active metamaterial. Precise control of the polarization response of a meta-material requires engineering not only the optical activity (circular birefringence), but also the linear birefringence which is often comparable or greater in magnitude. In the case of the semi-circular scatterer considered above the optical activity and linear birefringence effects are roughly equal in magnitude (Figure 3(b)). The desired polarization response of a given structure may often be found at a single frequency where contributions of multiple resonances add up favorably. For example in (15) attenuation of linear birefringence (pure optical activity) was achieved by examining the resonant response of the meta-material and identifying a single frequency in which linear birefringence is suppressed while the optical activity is maintained. An alternative more

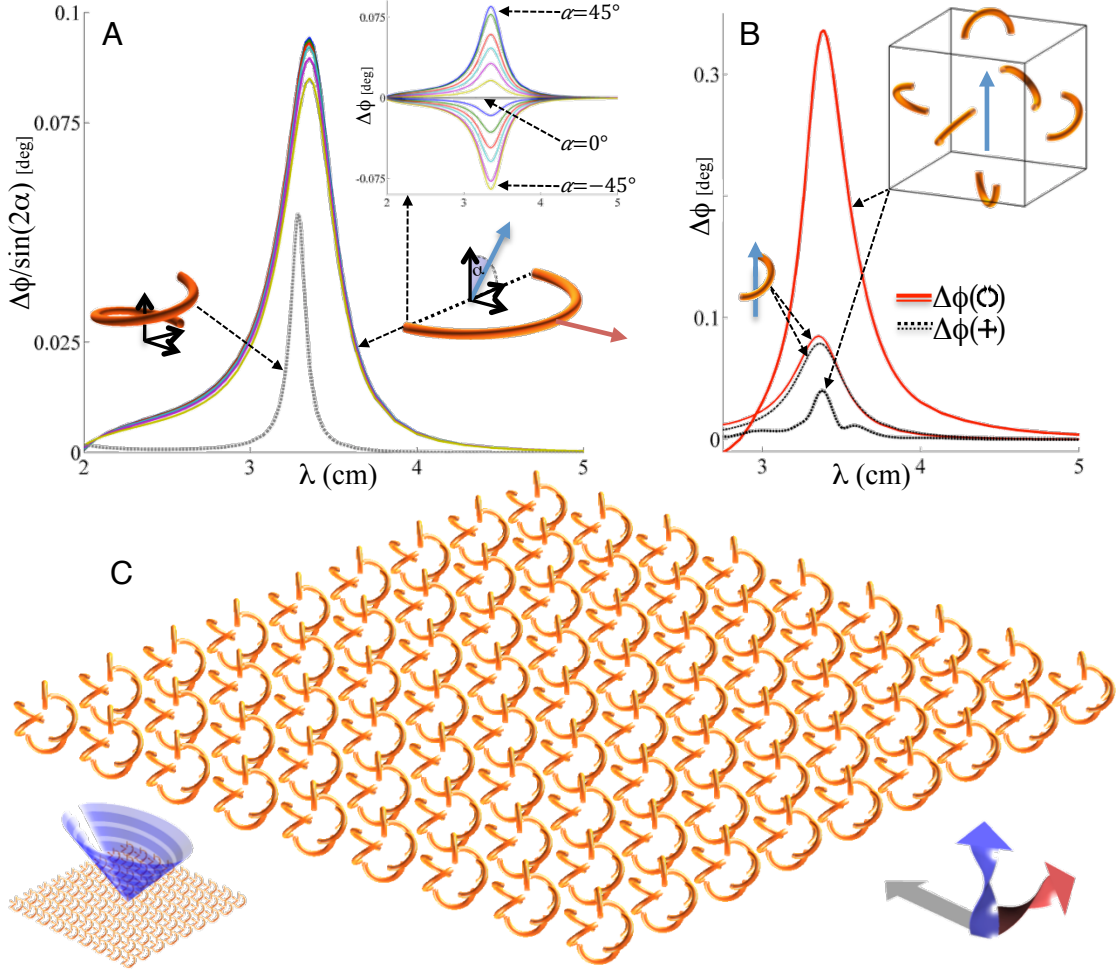


FIG. 3 *Optical activity and the design of an optically active mirror symmetric array of conducting scatterers* **(a)** The optical activity (relative phase delay between right and left circular polarizations) of a semicircular conducting wire calculated numerically at varying angles of incidence and plotted against the exciting wavelength (see methods). The peak response is observed at a wavelength $\lambda/2 \sim l$, where $l \sim \pi/2 \text{ cm}$ is the length of the scattering wire. The orientation of the semicircles is prescribed by a director (axis) which joins the semicircle's ends (dotted line), and a polar vector, \mathbf{p} , perpendicular to the director and pointing to the midpoint of the semicircle. The angle of incidence, α , is measured between the incident k vector and the normal to the semicircle. α is varied by rotating the semicircle about its polar vector. The strong angular dependence of the response amplitude (inset) is predicted by (1) to scale as $\sin(2\alpha)$ at all wavelengths, as observed by the collapse of the rescaled curves. The optical activity of a single period of a helix of the same length is given for comparison (dashed curve). The small discrepancy between the rescaled curves is due to a small fourth order tensor corrections, which can be calculated explicitly. See Supplementary Information. **(b)** To reduce linear birefringence of a single scatterer (thin black curve) while retaining its optical activity (thin red curve) we make use of the tensorial form of the optical activity (see appendix for the symmetry arguments). This allows a mirror symmetric arrangement of six semicircles on the faces of a cube such that both their directors and polar vectors are isotropically distributed, while retaining a constructive chiral response. The relative magnitude between the resulting optical activity (thick red curve) and the linear birefringence (thick black curve) is reduced by a factor ~ 8 . As the array of scatterers possess the same symmetry properties as a single scatterer, an array of arrays may be constructed to further diminish linear effects. Successive iteration will result in a hierarchical arrangement of scatterers exhibiting an exponential (in the iteration number) attenuation of linear birefringence and dichroism effects.

geometric route follows from the distinct transformation rules implied by the pseudo-tensorial structure of the the optical activity response. While linear birefringence is expected to change sign when the scatterer is rotated

by $\pi/2$ about the k vector direction, the optical activity is expected to remain unchanged by this rotation. To diminish the linear birefringence response in all directions one may attempt to impose this symmetry in

all directions. However this also results in the vanishing of the optical activity pseudo-tensor. By contrast, isotropically orienting the scatterer polar vector and director independently (as done in Figure 3), is less restrictive, and allows for a constructive chiral response. We implement this principle to design a spatial arrangement of six semi-circular scatterers that attenuates the linear birefringence while retaining the optical activity (Figure 3(b)). This arrangement constitutes a unit cell which, similarly to its semi-circular building blocks, is mirror symmetric making it possible to use the same principle to construct a hierachal bulk of scatterers.

When addressed in specific orientations, the physical objects considered above have a clear handedness that can manifest itself in chiral behavior, for example inducing rotation in a fluid or rotating the polarization of optical beams. This behaviour is captured uniquely, in each case, by a pseudo-tensor that relates a *direction* and a *rotation*. Additional measures can be constructed for additional physical situations. For example in the appendix we construct a chirality tensor describing 3D vector fields and a chirality tensor describing 1D embedded curves. Pseudo-tensorial quantifications of specific chiral phenomena have further been used in the context of optics (17; 18) and liquid crystals (12). While each physical manifestation of handedness may require a different chirality measure, we argue that in the general case, as they relate directions to rotations, all measures need be pseudo-tensorial.

It is important to note that while in some handed phenomena the descriptions of the handed response by a rank two tensor is exact , e.g. viscous (stokes) flow (13), there are chiral phenomena for which this is not the case. In the general case the chiral response $\mathcal{X}(\hat{\mathbf{n}}, \hat{\mathbf{r}})$ relating the direction $\hat{\mathbf{r}}$ and the rotation $\hat{\mathbf{n}}$ can be formally expanded in a series of higher rank pseudo-tensors. For example, in SM10 we derive for the collapse in Figure 3 the correction to the second rank tensor structure up to rank four tensors.

Upon taking the isotropic average of chirality tensors, which is physically equivalent to computing the average chiral response of a collection of randomly oriented copies of the object, as might occur for molecules in a solution, we recover a pseudo-scalar (the trace) that is consistent with chiral measures based on Kelvin's definition. However, for single objects, or aligned collections of objects, tensorial measures predict chiral behavior that depends on their orientation. We suggest that such tensorial measures provide a natural extension of Kelvin's definition of chirality itself.

Objects to which we can intuitively assign handedness, typically possess a well defined axis, rendering them amenable to the application of some variant of the right hand rule. In the tensorial sense, the object's axis serves

to single out one component of the tensor. If the same criteria for handedness are applied to perpendicular directions the remaining components may be obtained. Mirror symmetric objects are found to be not necessarily achiral (display no handedness), but rather amphichiral, capable of possessing equal amounts of right handedness and left handedness in perpendicular directions.

The tensorial quantification of chirality opens new avenues for the design of chiral objects and the manipulation of their chiral response. This gain however does not come without a cost; The handedness of a general object can no longer be simply stated by a single identifier e.g. “right handed”, and an oriented statement such as “isotropically left handed” or “uniaxially right handed” take its place. In the most general case one must resort to the use of tensors to fully capture the chirality of an object.

Appendix A: Chirality pseudo-tensor for embedded surfaces

In this appendix we construct the pseudo tensor χ^e that measures the rotation of a surface's normal in different directions. This tensor is similar in spirit to the helicity tensor proposed in (12; 19) in the context of nematic ordering by chiral probes. We consider a surface \mathbf{r} parameterized by the coordinates x^α , where $\alpha = 1, 2$. These coordinates induce the metric $a_{\alpha\beta} = \partial_\alpha \mathbf{r} \cdot \partial_\beta \mathbf{r}$, and the second fundamental form $b_{\alpha\beta} = \partial_\alpha \partial_\beta \mathbf{r} \cdot \hat{\mathbf{N}}$, where $\hat{\mathbf{N}}$ is the surface's normal. Given a direction in space $\hat{\mathbf{n}}$ with cartesian component n_i we project it to the surface's tangent space by

$$\hat{\mathbf{n}}_\parallel = (\partial_\beta \mathbf{r} \cdot \hat{\mathbf{n}}) a^{\alpha\beta} \partial_\alpha \mathbf{r}.$$

Differentiating a function f defined on the surface along the projection of $\hat{\mathbf{n}}$ reduces to

$$(\hat{\mathbf{n}}_\parallel \cdot \nabla) f = (\partial_\beta \mathbf{r} \cdot \hat{\mathbf{n}}) a^{\alpha\beta} \partial_\alpha f.$$

For an oriented derivative of a vector field $(\hat{\mathbf{n}} \nabla) \mathbf{V}$ we may isolate the component which is due to a pure rotation about a vector $\hat{\mathbf{m}}$ by the scalar product $\hat{\mathbf{m}} \cdot (\hat{\mathbf{N}} \times (\hat{\mathbf{n}} \nabla) \mathbf{V})$. Whenever this product is positive the change in the field \mathbf{V} along $\hat{\mathbf{n}}$ is associated with a right handed rotation about $\hat{\mathbf{m}}$. The rotation of the normal of a surface about a vector $\hat{\mathbf{m}}$ when displaced along the direction induced by the vector $\hat{\mathbf{n}}$ is then given by

$$\hat{\mathbf{m}} \cdot (\hat{\mathbf{N}} \times ((\partial_\beta \mathbf{r} \cdot \hat{\mathbf{n}}) a^{\alpha\beta} \partial_\alpha \hat{\mathbf{N}})) = \hat{\mathbf{m}} \chi^e \hat{\mathbf{n}}, \quad (\text{A1})$$

where the chirality density, χ^e , defined by equation (A1) can be rewritten in component form as

$$\chi_{ij}^e = \partial_\alpha r_j a^{\alpha\beta} \epsilon_{ilk} N^l \partial_\beta N^k, \quad (\text{A2})$$

where r_j and N^k denote the cartesian components of \mathbf{r} and $\hat{\mathbf{N}}$ and ϵ is the antisymmetric Levi-Civita tensor. We

may eliminate the normal vector from the formulation with the aid of the components of the second fundamental form $b_{\alpha\beta}$ and the two dimensional Levi Civita tensor $\epsilon_{\delta}^{\gamma}$:

$$\chi_{ij}^e = \partial_{\alpha} r_j \partial_{\delta} r_i a^{\alpha\beta} b_{\gamma\beta} \epsilon_{\delta}^{\gamma} / \sqrt{|a|}$$

It is easy to show that the chirality density above transforms as a pseudo-tensor and is independent of the surface's parametrization and of the sign of the normal vector.

Appendix B: Chirality pseudo-tensor for 3D director fields and unit vector fields

Let \mathbf{u} be a unit vector field in \mathbb{R}^3 such as the director of a nematic or cholesteric mesophase of a liquid crystal. Inspired by the normal rotation tensor for embedded surfaces we may ask for every two vectors $\hat{\mathbf{n}}$ and $\hat{\mathbf{m}}$ how does the unit vector field \mathbf{u} rotate about the vector $\hat{\mathbf{m}}$ when displaced along the direction $\hat{\mathbf{n}}$. In components this takes the form

$$n^i \chi_{ij} m^j = n^i \partial_i u^k \epsilon_{jkl} u^l m^j.$$

The trace of the chirality tensor defined above gives

$$\chi^{ii} = \partial_i u^k \epsilon_{ikl} u^l = (\nabla \times \mathbf{u}) \cdot \mathbf{u},$$

which coincides with the expression for helicity, c.f. magnetic helicity ($\mathbf{A} \cdot \mathbf{B} = \mathbf{A} \cdot (\nabla \times \mathbf{A})$), and hydrodynamic helicity ($\mathbf{u} \cdot \boldsymbol{\omega} = \mathbf{u} \cdot (\nabla \times \mathbf{u})$). Note that as the chirality density is quadratic in the unit vector field \mathbf{u} it remains unchanged under the transformation $\mathbf{u} \rightarrow -\mathbf{u}$ and therefore also applies to director fields. For example a simple cholesteric order in which the director field is given by

$$\mathbf{N} = (\cos(pz), \sin(pz), 0),$$

displays a uniaxial chirality density oriented along the z direction

$$\chi = \begin{pmatrix} 0 & 0 & 0 \\ 0 & 0 & 0 \\ 0 & 0 & -p \end{pmatrix}.$$

In general, when this chirality measure is applied to director fields it yields not only the degree of handedness (such as the cholesteric pitch above), but also associates the handed phenomena with a direction.

Appendix C: Chirality pseudo-tensor for embedded curves

Following again the same guiding principles which resulted in the chirality measure for embedded surfaces we come to examine the chirality of embedded curves. We construct the chirality density tensor χ_{ij} similarly so that the contraction $\mathbf{m}\chi\mathbf{n}$ gives the rate of rotation of the

curve's normal vector, \mathbf{N} , about the direction \mathbf{m} when displaced along the curve in the direction and magnitude projected from \mathbf{n} .

Let \mathbf{t}, \mathbf{N} and \mathbf{b} be a curve's tangent vector, normal vector and Binormal vector respectively. These unit vectors satisfy the Serret-Frenet formulas:

$$\partial_s \begin{pmatrix} \mathbf{t} \\ \mathbf{N} \\ \mathbf{b} \end{pmatrix} = \begin{pmatrix} 0 & \kappa & 0 \\ -\kappa & 0 & \tau \\ 0 & -\tau & 0 \end{pmatrix} \begin{pmatrix} \mathbf{t} \\ \mathbf{N} \\ \mathbf{b} \end{pmatrix},$$

where s is the arc-length parametrization of the curve and κ and τ are the curves curvature and torsion. Differentiating along the curve in direction projected from \mathbf{n} gives a weighted arc-length derivative $\mathbf{t} \cdot \mathbf{n} \partial_s$. The chirality density tensor may be simplified by the Serret-Frenet equations to read

$$\chi_{ij} = t_i \epsilon_{jlk} N^l \partial_s N^k = t_i t_j \tau + t_i b_j \kappa. \quad (\text{C1})$$

The trace of the chirality density gives the local torsion, $\chi_{ii} = \tau$. For locally planar curves where $\tau = 0$ this gives a traceless tensor, as expected from the local mirror symmetry of such curves. In the general case, however, the measure is not traceless. For example when considering a helicoid oriented along the z axis of pitch p ,

$$\mathbf{r} = (R \cos(\frac{s}{\sqrt{R^2 + p^2}}), R \sin(\frac{s}{\sqrt{R^2 + p^2}}), \frac{ps}{\sqrt{R^2 + p^2}}),$$

then for an integer number of windings, M , the integrated chirality tensor is uniaxial and oriented along the axis of the helicoid:

$$\mathcal{X} = \begin{pmatrix} 0 & 0 & 0 \\ 0 & 0 & 0 \\ 0 & 0 & \frac{2\pi M p}{\sqrt{R^2 + p^2}} \end{pmatrix} = \begin{pmatrix} 0 & 0 & 0 \\ 0 & 0 & 0 \\ 0 & 0 & \Delta Z \end{pmatrix},$$

where ΔZ is the height of the helicoid.

Appendix D: Optically active, isotropic and mirror symmetric collection of semicircular wire segments

We describe the orientation of a semicircular scatterer in space using a vector \mathbf{p} , pointing from the center of the semicircle to the midpoint on the wire segment, and a director \mathbf{d} (non-oriented vector, i.e. $\mathbf{d} = -\mathbf{d}$), which connects the segment's endpoints. If the scatterers are isotropically oriented then both optical activity and linear birefringence vanish. However, one can place six scatterers on the faces of a cube such that their polar vectors, \mathbf{p} , are isotropically oriented and their directors, \mathbf{d} , are also isotropically oriented, but such that their chirality tensors add constructively. Moreover this arrangement can be made to be symmetric under reflection, i.e. there exists an improper rotation, T , (a combination of an inversion and a rotation) which maps the arrangement of scatterers to itself.

The above arrangement is possible due to the difference in transformation rules between the different quantities; whereas \mathbf{p} and \mathbf{r} transform as vectors ($p'_i = \Lambda_i^j p_j$), χ transforms as a rank two pseudo-tensor ($\chi'_{ij} = -\Lambda_i^n \lambda_j^m \chi_{mn}$). The transformation T , mapping the scatterers arrangement to itself is given explicitly by $x \rightarrow -x, y \rightarrow -z$ and $z \rightarrow y$, and its transformation gradient given by

$$\Lambda = \begin{pmatrix} -1 & 0 & 0 \\ 0 & 0 & 1 \\ 0 & -1 & 0 \end{pmatrix}.$$

With the aid of this mapping and its transformation gradient we list in table I. the positions and orientations of the semicircular scatterers, alongside their positions and orientations after the application of the transformation T and show that their chirality tensors add constructively.

REFERENCES

- [1] Baron Kelvin, W. T. *Baltimore lectures on molecular dynamics and the wave theory of light*. C.J. Clay and Sons, London, 1904.
- [2] N. Weinberg and K. Mislow. A unification of chirality measures. *Journal of Mathematical Chemistry*, 17(1):35–53, 1995. WOS:A1995RD07400003.
- [3] P. W. Fowler. Quantification of chirality: Attempting the impossible. *Symmetry: Culture and Science*, 16(4):321–334, 2005.
- [4] S. Nonaka, H. Shiratori, Y. Saijoh, and H. Hamada. Determination of leftright patterning of the mouse embryo by artificial nodal flow. *Nature*, 418(6893):96–99, July 2002.
- [5] R. P Feynman, R. B Leighton, and M. Sands. *The Feynman lectures on physics. Vol. 1, chapter 52*. Addison-Wesley Publishing Co., Inc., Reading, Mass.-London, 1963.
- [6] J. P. Straley. Theory of piezoelectricity in nematic liquid crystals, and of the cholesteric ordering. *Physical Review A*, 14(5):1835–1841, November 1976.
- [7] A. Harris, R. Kamien, and T. Lubensky. Molecular chirality and chiral parameters. *Reviews of Modern Physics*, 71(5):1745–1757, 1999.
- [8] G. Millar, N. Weinberg, and K. Mislow. On the OsipovPickupDunmur chirality index: why pseudoscalar functions are generally unsuitable to quantify chirality. *Molecular Physics*, 103(20):2769–2772, October 2005.
- [9] A. B. Buda and K. Mislow. A hausdorff chirality measure. *J. Am. Chem. Soc.*, 114(15):6006–6012, 1992.
- [10] H. Zabrodsky and D. Avnir. Continuous symmetry measures. 4. chirality. *Journal of the American Chemical Society*, 117(1):462–473, January 1995.
- [11] S. Armon, E. Efrati, R. Kupferman, and E. Sharon. Geometry and mechanics in the opening of chiral seed pods. *Science*, 333(6050):1726 –1730, 2011.
- [12] A. Ferrarini and P. L. Nordio. On the assessment of molecular chirality. *Journal of the Chemical Society, Perkin Transactions 2*, (2):455–460, 1998.
- [13] E. M. Purcell. Life at low reynolds number. *American Journal of Physics*, 45(1):3, 1977.
- [14] M. V. Hobden. Optical activity in a non-enantiomorphous crystal silver gallium sulphide. 216(5116):678–678, November 1967.
- [15] E. Plum, V. A. Fedotov, and N. I. Zheludev. Optical activity in extrinsically chiral metamaterial. *Applied Physics Letters*, 93:191911, 2008.
- [16] L. E. Hough, M. Spannuth, M. Nakata, D. A. Coleman, C. D. Jones, G. Dantigraber, C. Tschiesske, J. Watanabe, E. Krblova, D. M. Walba, J. E. MacLennan, M. A. Glaser, and N. A. Clark. Chiral isotropic liquids from achiral molecules. *Science*, 325(5939):452–456, July 2009.
- [17] L. D. Barron. *Molecular Light Scattering and Optical Activity*. Cambridge University Press, 2 edition, November 2004.
- [18] L. D. Landau, L. P. Pitaevskii, and E. M. Lifshitz. *Electrodynamics of Continuous Media, Second Edition: Volume 8*. Butterworth-Heinemann, 2 edition, January 1984.
- [19] A. Ferrarini, G. J. Moro, and P. L. Nordio. Simple molecular model for induced cholesteric phases. *Physical Review E*, 53(1):681–688, January 1996.
- [20] R. C. Jones. A new calculus for the treatment of optical systems. VII. properties of the n-matrices. *JOSA*, 38(8):671683, 1948.
- [21] N. Weinberg and K. Mislow. On chirality measures and chirality properties. *Canadian Journal of Chemistry* 78, 4145 (2000).
- [22] O. Arteaga and A. Canillas. Analytic inversion of the Mueller-Jones polarization matrices for homogeneous media.

TABLE I Transformations of the spatial location \mathbf{r} , polar vector, \mathbf{p} , director, \mathbf{d} , and chirality tensors, χ for the optically active and reflection symmetric arrangement of scatterers

\mathbf{r}	\mathbf{p}	\mathbf{d}	$(\chi_{xx}, \chi_{yy}, \chi_{zz})$	$T(\chi_{xx}, \chi_{yy}, \chi_{zz})$	$T\mathbf{p}$	$T\mathbf{d}$	$T\mathbf{r}$
$(L, 0, 0)$	\mathbf{x}	$\mathbf{y} + \mathbf{z}$	$(0, 1, -1)$	$(0, 1, -1)$	$-\mathbf{x}$	$\mathbf{y} - \mathbf{z}$	$(-L, 0, 0)$
$(-L, 0, 0)$	$-\mathbf{x}$	$\mathbf{y} - \mathbf{z}$	$(0, 1, -1)$	$(0, 1, -1)$	\mathbf{x}	$\mathbf{y} + \mathbf{z}$	$(L, 0, 0)$
$(0, L, 0)$	\mathbf{y}	$\mathbf{x} - \mathbf{z}$	$(1, 0, -1)$	$(-1, 1, 0)$	$-\mathbf{z}$	$\mathbf{x} + \mathbf{y}$	$(0, 0, -L)$
$(0, 0, -L)$	$-\mathbf{z}$	$\mathbf{x} + \mathbf{y}$	$(-1, 1, 0)$	$(1, 0, -1)$	$-\mathbf{y}$	$\mathbf{x} + \mathbf{z}$	$(0, -L, 0)$
$(0, -L, 0)$	$-\mathbf{y}$	$\mathbf{x} + \mathbf{z}$	$(1, 0, -1)$	$(-1, 1, 0)$	\mathbf{z}	$\mathbf{x} - \mathbf{y}$	$(0, 0, L)$
$(0, 0, L)$	\mathbf{z}	$\mathbf{x} - \mathbf{y}$	$(-1, 1, 0)$	$(1, 0, -1)$	\mathbf{y}	$\mathbf{x} - \mathbf{z}$	$(0, L, 0)$

SUPPLEMENTARY MATERIAL

SM1. CONSTRUCTION OF THE ELASTIC BI-LAYER

Two sheets of a super soft silicone rubber (30a Durometer) of thickness $1/32"$ were strained uniaxially by 25 percent and their edges temporarily fixed to rigid plates. A thin layer of silicone adhesive (Dow Corning 732) was applied to both sheets. The sheets were then pressed against each other while maintaining the uniaxial strain axes perpendicular. The silicone was allowed to cure for a week. The glued bi-layer shows a thickness of 2mm with a spatial variation of $\pm 20\%$ when released from the tensional frame.

SM2. 3D PRINTED HELICOID SEGMENTS IN AN AIRFLOW

Half period helicoids of width 2 cm , length $\pi\text{ cm}$ and thickness 0.2 cm constrained by 0.4 cm diameter and 11 cm long cylindrical axes were printed using a 3D printer (Objet Connex350TM). The constraint axes passed through the helicoid's center and were directed in perpendicular directions, along the helicoids length and tangent to the helicoid at its center.

SM3. OPTICAL ACTIVITY SIMULATIONS

We used a commercial method of moments (MoM) solver, *HFSS-IE*, to solve the near field scattering off a conducting solid (copper from the *HFSS* built in material library). The scatterer was centered on the origin which was chosen as the zero phase of the incident plane wave excitation. The exciting wave's wavelength was varied between 10 mm and 150 mm revealing a single resonance approximately at the scatterer's length. The semicircular ring of figure 3 is one half of a torus of minor radius 0.05 mm and a major radius of 5.05 mm , the helical segment is of the same wire thickness (0.05 mm), and a radius and pitch $r_0 = p \approx 2.4\text{ mm}$ resulting in the same overall wire length. A near field measurement at a distance of 2000 mm from the origin of the scattered field was added to the unattenuated incident plane wave. Two

linearly polarized incident wave calculations were used to obtain the different components of the Jones matrix. The linear and circular components of the birefringence were extracted under the assumption of a homogenous media as elaborated in appendix .

SM4. GEOMETRY OF THE ELASTIC BI-LAYER

Following [11] we identify the intrinsic geometry resulting from the construction of the bi-layer with a uniform first and second reference fundamental forms:

$$a = \begin{pmatrix} 1 & 0 \\ 0 & 1 \end{pmatrix}, \quad b = \begin{pmatrix} 0 & k \\ k & 0 \end{pmatrix},$$

where principal curvature directions coincide with the tension directions in each of the layers. The magnitude of the reference curvature may be calculated via $k = \frac{1}{\delta z} \frac{\alpha^2 - 1}{\alpha^2 + 1}$ where α is the uniaxial elongation factor with respect to the unstrained state. In our system $\alpha = 1.25$ and $\delta z \approx 1.4\text{ mm}$ is measured between the mid-surfaces of top and bottom layers which yields $k \approx 0.15 \frac{1}{\text{mm}}$.

SM5. THE MOST GENERAL FORM OF A MIRROR SYMMETRIC PSEUDO-TENSOR

Theorem: *The second rank chirality pseudo-tensor of mirror symmetric bodies is symmetric traceless and of vanishing determinant.*

Proof: Every rank two pseudo-tensor χ may be decomposed into a symmetric part, S , and an anti-symmetric part, A . We assume that there exists an improper rotation which leaves χ unaltered. We rewrite this improper rotation as an inversion (all coordinates changes sign), followed by an unknown, proper rotation O . Thus we may write $O^T \chi O = -\chi$ for some proper rotation O . We may rewrite this equality as

$$O^T S O + S = -O^T A O - A.$$

As the left hand side above is symmetric, and the right hand side is anti-symmetric, each of them has to vanish independently. By $O^T S O = -S$ we obtain that S has to

have vanishing determinant and trace. It therefore can be rotated to the form

$$S = c \begin{pmatrix} 1 & 0 & 0 \\ 0 & -1 & 0 \\ 0 & 0 & 0 \end{pmatrix}.$$

The proper rotation O may now be easily determined to be a rotation by $\pi/2$ about the z axis. When S is diagonalized, we assume A has the form

$$A = \begin{pmatrix} 0 & a & b \\ -a & 0 & c \\ -b & -c & 0 \end{pmatrix},$$

which upon application of the rotation O gives $a = b = c = -b = 0$.

S6. RESOLVING THE PARADOX OF CHIRAL CONNECTEDNESS

Chiral connectedness, the ability to continuously deform an object into its mirror image without passing through a configuration which is mirror symmetric stands at the heart of the inability to quantify chirality. The tensorial generalization to the quantification of handedness resolves the seeming contradiction generated by chiral connectedness in three different levels. First, a higher dimensional object (such as a tensor) can change sign without passing through zero as can be seen in Fig. SM.4 below. This notion, in the context of vectors, was discussed by Weinberg and Mislow soon after the discovery of chiral connectedness yet was discarded claiming that vectors do not allow simple ordering thus cannot form adequate chirality measures (21). Second, the reason to claim that the chirality tensor of a mirror symmetric object must vanish is because for pseudo-scalars and scalar measures if $\chi = -\chi$ then $\chi = 0$ necessarily. As displayed in the previous section this does not hold for pseudo-tensors. Thus, formally, the non-vanishing chirality tensors of mirror symmetric bodies does not stand in contradiction with Lord Kelvin's definition.

Third, the oriented quantification of chirality proposed here does not take the lack of mirror symmetry to be the source of handedness but defines handedness as the relation between directions and rotations. As such even non-mirror symmetric objects are allowed to display no handedness with respect to a specific given measure.

SM7. CHIRALITY PSEUDO-TENSOR FOR EMBEDDED SURFACES

Theorem: Let \mathbf{r} denote the smooth embedding of a surface into R^3 , and let $\mathcal{X} = \int \int \chi dA$ be a rank two chirality pseudotensor originating from a local rank two

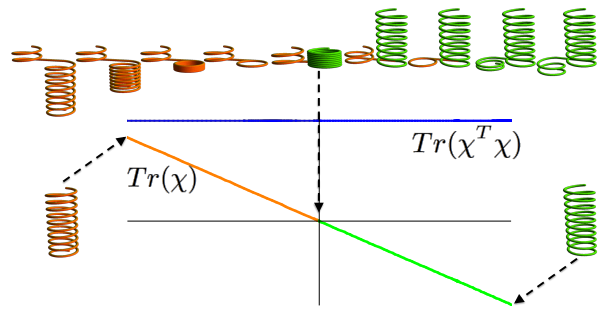


FIG. 4 *Chiral-connected path between a right handed helix and its left handed mirror image.* The first two isotropic invariants of the chirality tensor (calculated explicitly for the curve using the formula $\mathcal{X} = \int (\kappa t_i t_j + \tau t_i b_j) ds$ derived at the appendix of the main text) plotted against a parameter describing the continuous deformation of the right handed helix (orange) to the left handed helix (green). The first isotropic invariant, χ_{ii} , given by the green and orange line coincides with the scalar definition of chirality indices. This measure reads zero when the right handed portion of the helix and the left handed portion are the same height. This configuration is, however, not symmetric under reflections as the right handed portion is composed of two windings whereas the left handed portion is composed of eight windings. The second invariant, $\chi_{ij}\chi_{ij}$ (divided by 10 for graphical purposes), is plotted in blue and barely changes throughout the transformation. In particular it remains bound away from zero.

chirality density pseudo-tensor which depends only on first and second derivatives of \mathbf{r} , i.e. $\chi = \chi(\partial_\alpha \mathbf{r}, \partial_{\alpha\beta} \mathbf{r})$, then \mathcal{X} is traceless.

Proof: Given the first and second fundamental forms of a surface, a and b , then the surface they define is unique to within rigid motions. This implies that all scalars which are constructed from the first two derivatives of a surface must be expressible in terms of the metric, its first derivatives and the second fundamental form; $a_{\alpha\beta}$, $\partial_\gamma a_{\alpha\beta}$ and $b_{\alpha\beta}$. The trace of the chirality tensor, χ_{ii} , is such a scalar.

Locally, the structure of a smooth surface as given by the metric, its derivative and the first fundamental form is mirror symmetric with two mirror symmetry planes spanned by the normal to the plane and each of the directions of principal curvatures. This implies that one can always create a mirror symmetric environment to a point p such that the induced metric, the metric first derivatives and the second fundamental form will all coincide with that of the original surface. It follows that the trace of such a chirality density must describe the trace

of a mirror symmetric object, and thus vanish identically.

SM8. HIGHER RANK CHIRALITY PSEUDOTENSORS

The chirality quantification of the examples considered in the main text are dominated by rank two pseudotensors. In some cases such a second order quantification is exact. For example in viscous flows, due to the linearity of the the governing equations, there is a general linear relation between the velocity U and rotation Ω of a body in an otherwise quiescent viscous fluid and the force F and couple G applied to it through a resistance matrix [13]:

$$\begin{pmatrix} F \\ G \end{pmatrix} = \begin{pmatrix} A & L \\ L^T & B \end{pmatrix} \begin{pmatrix} U \\ \Omega \end{pmatrix}.$$

The off diagonal block L relating a given rotation to a linear force, as well as the combination $B^{-1}L^T$ which relates the rotation due to translation of a torque free body are both measures of chirality which are captured exactly by a rank two tensor.

The general case of chirality admits more complicated orientational structure. In such cases the chirality function which relates the direction $\hat{\mathbf{r}}$ with the rotation $\hat{\mathbf{n}}$, $\chi(\hat{\mathbf{n}}, \hat{\mathbf{r}})$, may be expanded in a formal tensor series

$$\begin{aligned} \chi(\hat{\mathbf{n}}, \hat{\mathbf{r}}) = & r^i \chi_{ij}^{1,1} n_j + r_i r_j \chi_{ijk}^{2,1} n_k + r_i r_j r_k \chi_{ijkm}^{3,1} n_m \\ & + r_i \chi_{ijkm}^{1,3} n_j n_k n_m + \dots \end{aligned}$$

The higher order tensorial corrections may be calculated directly as done below (in S.10). It is important to note, however, that in some cases symmetry sets the second rank tensor to zero and the dominant behavior is governed by a higher rank tensor. This is the case of the four cup anemometer which is designed to spin about the z-axis in the same fashion for both wind from the x direction and from the $-x$ direction. The lowest order pseudotensor which is capable of such a response is the rank three $\chi^{2,1}$.

SM9. OPTICAL ACTIVITY EXTRACTION

Monochromatic scattering is described by a Jones matrix relating the incident and scattered plane wave components:

$$\begin{pmatrix} E_x^{out} \\ E_y^{out} \end{pmatrix} = \begin{pmatrix} J_{xx} & J_{xy} \\ J_{yx} & J_{yy} \end{pmatrix} \begin{pmatrix} E_x^{in} \\ E_y^{in} \end{pmatrix}$$

Following Jones (20), we identify the four independent complex entries of the Jones matrix, J , with the eight independent polarization transformations: *i.* A global

phase retardation and amplitude attenuation, *ii.* Circular dichroism and circular birefringence, *iii.* Linear birefringence and linear dichroism in the (x, y) linear polarizations, and *iv.* Linear birefringence and linear dichroism in the $(x+y, x-y)$ linear polarizations. As the different Jones matrices associated with the different polarization phenomena do not commute, a decomposition of a Jones matrix to a product of such "pure" components will not be unique, and the values associated with the strength of each phenomena will depend on the order of the elements in the product. If, however, we consider the generators of the polarization effects, then to linear order, the result does not depend on the order in which they are summed. Conceptually this amounts to decomposing the medium to infinitesimal laminae each displaying one of the polarization effects. As their thickness is infinitesimal the order in which these laminae are placed one after the other does not change the result. This assumption of a homogenous medium results in the following interpretation of the Jones matrix components.

$$J = e^{-i\eta/2} \begin{pmatrix} \cos(\frac{T}{2}) - i\frac{L}{T} \sin(\frac{T}{2}) & \frac{C-i\tilde{L}}{T} \sin(\frac{T}{2}) \\ -\frac{C+i\tilde{L}}{T} \sin(\frac{T}{2}) & \cos(\frac{T}{2}) + i\frac{L}{T} \sin(\frac{T}{2}) \end{pmatrix},$$

where $T = \sqrt{L^2 + \tilde{L}^2 + C^2}$, $L = LB_{0,90} - i LD_{0,90}$ measures the linear birefringence and dichroism of the linear polarization along the x and y axes, $\tilde{L} = LB_{45,-45} - i LD_{45,-45}$ measures the linear birefringence and dichroism of the linear polarization along the $x+y$ and $x-y$ directions, $C = CB - i CD$ measures the circular birefringence and dichroism and η accounts for the isotropic amplitude attenuation and phase retardation (20; 22). For a weak scatterer the extraction of the optical activity form the Jones matrix, J , is unique.

SM10. ADDITIONAL OPTICAL ACTIVITY CALCULATIONS FOR A SINGLE SCATTERER

1. Tensorial structure along the perpendicular direction

Rank four chirality pseudo-tensor corrections

We compute the corrections up to rank 4 to the optical activity of the single scatterer considered in figure 3 of the main text. As in the case of the rank 2 tensor for a mirror symmetric object , symmetries serve to reduce the number of independent entries.

For the rank three tensor we obtain that the non vanishing components are $\chi_{\{123\}}^{2,1}$ and $\chi_{\{132\}}^{2,1}$ where $\{123\}$ denote all possible cyclic index permutations, i.e $((123), (231), (312))$. For the rank four tensor the only non vanishing components are:

$$\chi_{\{1113\}}^{3,1}, \quad \chi_{\{3331\}}^{3,1}, \quad \chi_{\{2123\}}^{3,1}, \quad \chi_{\{2231\}}^{3,1}, \quad \chi_{\{2213\}}^{3,1}.$$

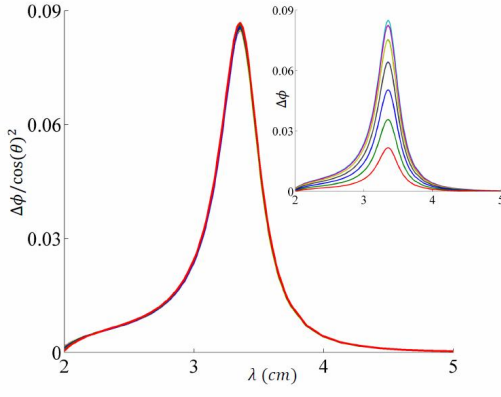


FIG. 5 *The tensorial structure of the optical activity response*
The semicircular scatterer of figure 3 of the main text is oriented in the direction of maximal response ($\alpha = 45^\circ$) and rotated about its director (the line connecting its endpoints) from $\theta = -30^\circ$ to $\theta = 60^\circ$ at 10° intervals. The optical activity angular dependence (inset) is expected to follow a simple projection rule and display a $\cos(\theta)^2$ dependence as observed by the collapse of the curves.

We note that for optical activity calculations, where the \mathbf{k} vector serves as both the direction of propagation and the axis of rotation, $\chi^{1,3}$ and $\chi^{3,1}$ relate to the same tensor thus only one of them needs to be prescribed. In particular, when contracted with a single vector $\mathbf{k} = (\cos(\alpha), 0, \sin(\alpha))$, we obtain

$$\begin{aligned} k^i k^j \chi_{ij}^{1,1} &= \cos(\alpha) \sin(\alpha) (\chi_{13}^0 + \chi_{31}^0), \\ k^i k^j k^l \chi_{ijl}^{2,1} &= 0, \\ k^i k^j k^l k^n \chi_{ijln}^{3,1} &= \cos(\alpha) \sin(\alpha) \times \\ &\quad (\cos^2(\alpha) (\chi_{1333}^{3,1} + \chi_{3133}^{3,1} + \chi_{3313}^{3,1} + \chi_{3331}^{3,1}) \\ &\quad + \sin^2(\alpha) (\chi_{3111}^{3,1} + \chi_{1311}^{3,1} + \chi_{1131}^{3,1} + \chi_{1113}^{3,1})) \\ &= \cos(\alpha) \sin(\alpha) (A_1 \cos(2\alpha) + A_2), \end{aligned} \quad (1)$$

where A_1 and A_2 are independent of α . Subtracting the curves rescaled by $\cos(\alpha) \sin(\alpha)$ observed in Figure 3 in the main text from the curve of maximal response results in the curves observed below in Fig. SM. 6 which scale as $\cos(2\alpha)$. We note that this collapse also displays a 5 percent variation which may be attributed to even higher order corrections.

SM11. OPTICAL ACTIVITY IN CONTINUOUS MEDIA: THE ELECTRO GYRATION TENSOR

Optical activity in weakly dispersive continuous media can be described by the electro-gyration tensor, g , appearing in the spatial variation of the dielectric per-

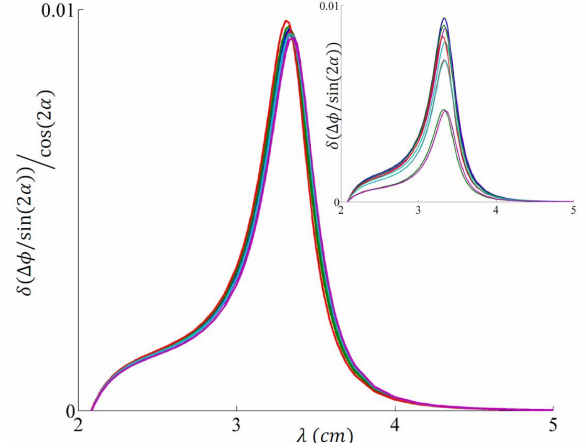


FIG. 6 *Rank four tensor corrections to the optical activity*
The difference between the collapsed curves in figure 3 of the main text is observed mostly around the resonant peak, and is about an order of magnitude smaller than the peak value (inset). Further calculation shows that the symmetry of the problem allows no non-trivial rank three pseudotensors, and restricts the form of the rank four tensors to display a $\cos(2\alpha)$ angular dependence as observed by the collapse of the rescaled curves.

mittivity tensor

$$\varepsilon_{ij} = \varepsilon_{ij}^0 + i \frac{c}{\omega} \epsilon_{ijk} g_{kl} k_l,$$

where k_l are the components of the wave vector, ϵ_{ijk} is the antisymmetric Levi-Civita pseudo-tensor and both ε^0 and g may depend on frequency. The right hand side of the equation above may be interpreted as an expansion in \mathbf{k} of the dielectric tensor [18]. A natural (and common) path is to identify the eigenmodes of the above dispersion relation and their corresponding refractive indices. For a monochromatic plane wave the combination of Maxwell's equations

$$\nabla \times (\nabla \times \mathbf{E}) = -\frac{1}{c^2} \ddot{\mathbf{D}} \quad (2)$$

may be recast in the following form

$$n^2 E_i - n_i (n_j E_j) = D_i = \varepsilon_{ij} E_j,$$

where $\mathbf{n} = c\mathbf{k}/\omega$. The desired plane wave eigenmodes form the null space of

$$n^2 \delta_{ij} - n_i n_j - \varepsilon_{ij} = n^2 \delta_{ij} - n_i n_j - \varepsilon_{ij}^0 - i \epsilon_{ijk} g_{kl} n_l.$$

For an isotropic medium $\varepsilon_{ij}^0 = \varepsilon^0 \delta_{ij} = n_0^2 \delta_{ij}$. Considering a plane wave propagating along the z direction we obtain to leading order in g

$$n_z^2 = n_0^2 \pm g_{zz}.$$

The polarization which correspond to these values are:

$$E_y = \mp i E_x,$$

which correspond to circular polarizations.

While the above analysis is very powerful, a linearly polarized plane wave ansatz yields a clearer interpretation of the gyration tensor g . Let us consider a plane wave solution of the form

$$\mathbf{E} = e^{i\omega t} \mathbf{P}(\mathbf{k}_0 \cdot \mathbf{r}) e^{i\mathbf{k}_0 \cdot \mathbf{r}}, \quad (3)$$

where $\mathbf{k}_0 = n_0 \omega / c \hat{z} = \sqrt{\epsilon_0} \omega / c \hat{z}$. Substituting this form into (2) we obtain to leading order in g the propagation equation for the x, y polarization vector

$$\mathbf{P}'(k_0 \cdot r) = -ig_{zz} \frac{1}{2n_0^2} \sigma_y \mathbf{P}(k_0 \cdot r)$$

where $\mathbf{P} = \begin{pmatrix} P_x \\ P_y \end{pmatrix}$, and $\sigma_y = \begin{pmatrix} 0 & -i \\ i & 0 \end{pmatrix}$ is the second Pauli matrix. We may therefore interpret in the general case the component $\hat{\mathbf{k}}^T g \hat{\mathbf{k}}$ as the scalar multiplier of the generator of linear polarization rotation in the direction of propagation.